Title	Pulsed laser diode based desktop photoacoustic tomography for monitoring wash-in and wash-out of dye in rat cortical vasculature
Author(s)	Kalva, Sandeep Kumar; Upputuri, Paul Kumar; Rajendran, Praveenbalaji; Dienzo, Rhonnie Austria; Pramanik, Manojit
Citation	Kalva, S. K., Upputuri, P. K., Rajendran, P., Dienzo, R. A., & Pramanik, M. (2019). Pulsed laser diode based desktop photoacoustic tomography for monitoring wash-in and wash-out of dye in rat cortical vasculature. Journal of Visualized Experiments, (147). doi:10.3791/59764
Date	2019
URL	http://hdl.handle.net/10220/48791
Rights	

Video Article

Pulsed Laser Diode-Based Desktop Photoacoustic Tomography for Monitoring Wash-In and Wash-Out of Dye in Rat Cortical Vasculature

Sandeep Kumar Kalva[1], Paul Kumar Upputuri[1], Praveenbalaji Rajendran[1], Rhonnie Austria Dienzo[1], Manojit Pramanik[1]

[1]School of Chemical and Biomedical Engineering, Nanyang Technological University

Correspondence to: Manojit Pramanik at manojit@ntu.edu.sg

URL: https://www.jove.com/video/59764
DOI: doi:10.3791/59764

Keywords: Bioengineering, Issue 147, acoustic reflector, single-element ultrasound transducer, photoacoustic imaging, photoacoustic tomography, pulsed laser diode, multiple ultrasound transducers, small animal imaging

Date Published: 5/30/2019

Citation: Kalva, S.K., Upputuri, P.K., Rajendran, P., Dienzo, R.A., Pramanik, M. Pulsed Laser Diode-Based Desktop Photoacoustic Tomography for Monitoring Wash-In and Wash-Out of Dye in Rat Cortical Vasculature. *J. Vis. Exp.* (147), e59764, doi:10.3791/59764 (2019).

Abstract

Photoacoustic (PA) tomography (PAT) imaging is an emerging biomedical imaging modality useful in various preclinical and clinical applications. Custom-made circular ring array-based transducers and conventional bulky Nd:YAG/OPO lasers inhibit translation of the PAT system to clinics. Ultra-compact pulsed laser diodes (PLDs) are currently being used as an alternative source of near-infrared excitation for PA imaging. High-speed dynamic in vivo imaging has been demonstrated using a compact PLD-based desktop PAT system (PLD-PAT). A visualized experimental protocol using the desktop PLD-PAT system is provided in this work for dynamic in vivo brain imaging. The protocol describes the desktop PLD-PAT system configuration, preparation of animal for brain vascular imaging, and procedure for dynamic visualization of indocyanine green (ICG) dye uptake and clearance process in rat cortical vasculature.

Video Link

The video component of this article can be found at https://www.jove.com/video/59764/

Introduction

Photoacoustic computed tomography (PACT/PAT) is a promising non-invasive biomedical imaging modality combining rich optical contrast with high ultrasond resolution[1,2,3,4,5]. When a nanosecond pulsed laser deposits energy onto light absorbing chromophores present inside any biological tissue, local temperature increases leading to thermoelastic expansion and contraction of the tissue, resulting in generation of pressure waves. These pressure waves are known as ultrasound waves or photoacoustic (PA) waves, which can be detected by ultrasound transducers around the sample. The detected PA signals are reconstructed using various reconstruction algorithms[6,7,8,9] to generate cross-sectional PA images. PA imaging provides structural and functional information from macroscopic organs to microscopic organelles due to the wavelength dependence of endogenous chromophores present inside the body[10]. PAT imaging has been successfully used for breast cancer detection[1], sentinel lymph node imaging[11], mapping of oxyhemoglobin (HbO_2), deoxyhemoglobin (HbR), total hemoglobin concentration (HbT), oxygen saturation (SO_2)[12,13], tumor angiogenesis[14], small animal whole body imaging[15], and other applications.

Nd:YAG/OPO lasers are conventional excitation sources for first generation PAT systems that are widely used in photoacoustic community for small animal imaging and deep tissue imaging[16]. These lasers provide ~100 mJ energy pulses at low repetition rates of ~10-100 Hz. The PAT imaging systems using these costly and bulky lasers are not suitable for high-speed imaging with single-element ultrasound transducers (SUTs), due to the limited pulse repetition rate. This inhibits real-time monitoring of physiological changes occurring at high speeds inside the animal. Using array-based transducers like linear, semi-circular, circular, and volumetric arrays with Nd:YAG laser excitation, high-speed imaging is possible. However, these array transducers are expensive and provide lower sensitivities compared to SUTs; yet, the imaging speed is limited by the low repetition rate of the laser. State-of-the-art single-impulse PACT systems with customized full-ring array transducer obtain the PA data at 50 Hz frame rates[17]. These array transducers need complex back-end receiving electronics and signal amplifiers, making the overall system more expensive and difficult for clinical use.

Their compact size, lower cost requirements, and higher pulse repetition rate (order of KHz) make pulsed laser diodes (PLDs) more promising for real-time imaging. Due to these advantages, PLDs are actively used as an alternate excitation source in second generation PAT systems. PLD-based PAT systems have been demonstrated successfully for high-frame rate imaging using array transducers[18], deep-tissue and brain imaging[19,20,21], cardiovascular disease diagnosis[22], and rheumatology diagnosis[23]. As SUTs are highly sensitive and less expensive compared to array transducers, they are still extensively used for PAT imaging. Fiber-based PLD system have been demonstrated for phantom imaging[24]. A portable PLD-PAT system has been demonstrated previously by mounting the PLD inside the PAT scanner[25]. With one SUT circular scanner, phantom imaging was performed during 3 s of scan time, and in vivo rat brain imaging was performed during a 5 s period using this PLD-PAT system[19].

Furthermore, improvements have been made to this PLD-PAT system to make it more compact and create a desktop model using eight acoustic reflector-based single-element ultrasound transducers (SUTRs)[26,27]. Here, SUTs were placed in a vertical instead of horizontal direction with

the aid of a 90° acoustic reflector[28]. This system can be employed for scan times of up to 0.5 s and ~3 cm deep in tissue imaging and in vivo small animal brain imaging. In this work, this desktop PLD-PAT system is used to provide the visual demonstration of experiments for in vivo brain imaging in small animals and for dynamic visualization of uptake and clearance process of Food and Drug Administration (FDA)-approved indocyanine green (ICG) dye in rat brains.

Protocol

All animal experiments were performed according to the guidelines and regulations approved by the Institutional Animal Care and Use Committee of Nanyang Technological University, Singapore (Animal Protocol Number ARF-SBS/NIE-A0331).

1. System description

1. Mount the PLD laser into the circular scanner and mount the optical diffuser (OD) in front of the PLD exit window to make the output beam homogeneous, as shown in **Figure 1A**. Connect the PLD to the laser driver unit (LDU).
   NOTE: The PLD generates ~816 nm wavelength pulses, pulses of ~107 ns in duration, and up to a 2 KHz repetition rate with a maximum pulse energy of ~3.4 mJ. The LDU consists of chiller, 12 V power supply, variable high voltage power supply to control the laser power, and function generator to change the pulse repetition rate.
2. Mount all eight SUTRs on each SUTR holder one-by-one such that the surface of each acoustic reflector faces towards the center of the scanning area, as shown in **Figure 1B**. Connect each SUTR cable to the low-noise signal amplifier with the help of connecting cables.
   NOTE: The central frequency of the ultrasound transducer is 5 MHz and has a 13 mm diameter active area. Two amplifiers each of 24 dB gain are connected in series for each channel.
3. Switch on the power supply of the chiller, then turn on the switch of the chiller to set the temperature between 20 °C and 25 °C.
4. Switch on the supply of the low voltage power supply and slowly turn the current control to set the current limit at 0.3 A. Set the voltage to 12 V. Verify that the current does not exceed 0.1 A.
5. Switch on the supply of the high voltage power supply. Press the “Preset” button and set the current to 1 A and voltage to 0 V. Enable the “Output” button: 0 V/0 A.
6. Switch on the power supply of the function generator. Press the “Recall” button and choose a 2 KHz configuration to generate the laser pulses at this repetition rate.
7. Place acrylic tank inside the scanner as shown in **Figure 1A** and fill the tank with water such that the detecting surface of the SUTRs are immersed completely inside water.
8. Make sure all the SUTRs detecting surfaces are inside the water medium. Switch on the power supply of the low-noise-signal amplifier.

2. Animal preparation for rat brain imaging

NOTE: Healthy female rats (see **Table of Materials**) were used to demonstrate the above described desktop PLD-PAT system for imaging small animal cortical vasculature.

1. Hold the animal on its back by arresting the head and body motion. Anesthetize the animal by intraperitoneal injection of a mixture of 2 mL of ketamine (100 mg/mL), 2 mL of xylazine (20 mg/mL), and 1 mL of saline (dosage of 0.2 mL/100 g).
   NOTE: After the injection, the animal’s toe is pinched to test for any positive reflexes such as leg or body movements, vocalization, or marked increases in respirations. An absence of such reflex actions confirms successful anesthetization of the animal.
2. To prevent dryness due to anesthesia and laser illumination, very carefully apply artificial tear ointment to the rat eyes. Place the animal in prone position on the working bench and remove the fur on the scalp of the animal using a hair trimmer and gently apply hair removal cream to the shaved area and remove the fur completely.
   1. After 4–5 min, remove the applied cream using a cotton swab.
3. Mount the custom-made animal holder (see **Table of Materials**) equipped with a breathing mask (see **Table of Materials**) on a lab-jack.
4. Place the animal in prone position on the holder so that the head rests on the horizontal platform of the holder. Use surgical tape to secure the animal to the holder.
5. Ensure that the breathing mask covers the nose and mouth of the rat to deliver anesthesia mixture. The breathing mask is customized to suit the imaging window. 10% of the commercially available nose cone is cut and then connected to a piece of glove.
6. Connect the breathing mask to the anesthesia machine before switching it on.
7. Switch on the anesthesia machine and set it to deliver anesthetic mixture containing 1.0 L/min of oxygen with 0.75% isoflurane to the animal breathing mask.
   1. Clamp the pulse oximeter to one of the animal’s hind legs to monitor its physiological condition.
8. Apply a layer of colorless ultrasound gel to the scalp of the rat using a cotton tipped applicator. Adjust the lab-jack position to the center of the scanner and adjust the height of the lab-jack manually so that the imaging plane is at the center of the acoustic reflector.

3. Dynamic in vivo imaging of uptake and clearance process of ICG in rat brain

1. Set the parameters in the data acquisition software (see **Table of Materials**) for a 360° acquisition scan.
2. Turn on the PLD laser emission by enabling the output of the function generator (laser emission will start). Then, slowly increase the voltage of the variable high voltage power supply to 120 V for maximum per pulse energy.
3. Run the data acquisition software (see the **Table of Materials**) program to rotate all eight SUTRs in 360° over a 4 s scan time.
   NOTE: For example, if the SUTRs are rotated for 4s, the PLD delivers 8,000 (= 4 x 2,000) pulses and each SUTR collects 8000 A-lines. These 8,000 A-lines are reduced to 400 by averaging over 20 signals (after averaging A-lines = 8,000/20 = 400). A reconstruction program based on delay-and-sum back projection algorithm is used to find out the scanning radius of each SUTR.

4. Disable the output of the function generator to turn off the laser emission.
5. Using the reconstruction algorithm in data processing software (see **Table of Materials**) find out the scanning radius of all eight SUTRs by trial-and-error, using the back-projection algorithm.
6. Set the parameters in the data acquisition software (see **Table of Materials**) for 45° acquisition over a 0.5 s scan time.
   NOTE: For example, if the SUTRs are rotated for 0.5s, the PLD delivers 1,000 (= 0.5 x 2,000) pulses and each SUTR collects 1000 A-lines. These 1,000 A-lines are reduced to 400 by averaging over 20 signals (after averaging A-lines = 1,000/20 = 50).
7. Enable the output of the function generator to turn on the laser emission.
8. Run the data acquisition software (see **Table of Materials**) program to rotate all eight SUTRs in 45° to obtain initial control data before administering ICG.
9. Disable the output of the function generator to turn off the laser emission.
10. Identify the tail vein of the animal and inject 0.3 mL of ICG (see **Table of Materials**) (323 µM) into the tail vein of the rat.

4.

NOTE: 1.25 mg of ICG powder was weighed using a micro-weighing machine and mixed with 5 mL of distilled water to obtain a concentration of 323 µM for the ICG solution.

1. Enable the output of the function generator to turn on the laser emission.
2. Run the data acquisition software (see **Table of Materials**) program to acquire A-lines over a 0.5 s scan time in 45° rotation.

5.

NOTE: A-lines acquired during a 0.5 s scan time are used to generate one cross-sectional image. There is time gap of ~0.4–0.6 s between each scan.

1. After the data acquisition is over, using the back-projection algorithm in data processing software (see **Table of Materials**), reconstruct the cross-sectional brain image from the saved A-lines.
2. Turn off the laser and then turn off anesthesia machine, lower the lab-jack and remove the animal from the stage. Return the animal to the cage and monitor until it regains consciousness.

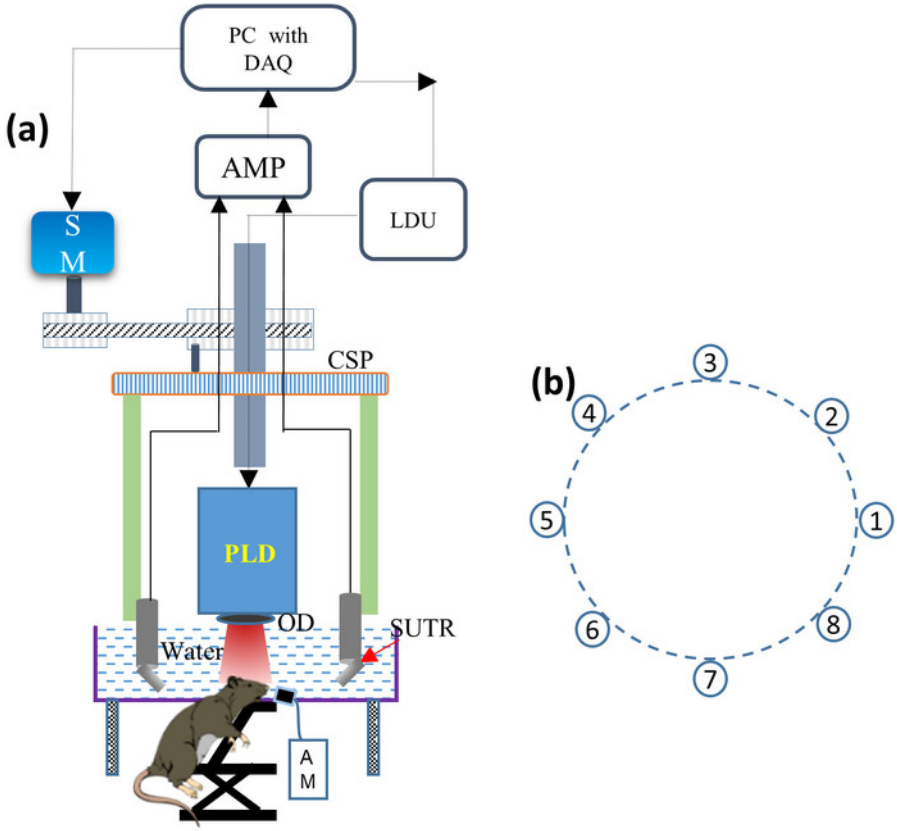

Figure 1: Schematic of the desktop PLD-PAT system. (**A**) Schematic of the desktop PLD-PAT set up. PLD: pulsed laser diode, OD: optical diffuser, SUTR: acoustic reflector based single-element ultrasound transducer, AM: anesthesia machine, CSP: circular scanning plate, SM: stepper motor, LDU: laser driving unit, AMP: amplifier, DAQ: data acquisition card. (**B**) Circular arrangement of eight SUTRs around the scanning center. Please click here to view a larger version of this figure.

Representative Results

The potentiality of the described desktop PLD-PAT system for dynamic in vivo brain imaging has been showcased in this protocol with corresponding results. High-speed imaging capability of the desktop PLD-PAT system was demonstrated by performing in vivo brain imaging of healthy female rats. PA signals were collected using eight SUTRs rotating in 360° and 45° around the rat brain at scan speeds of 4 s and 0.5 s, respectively. **Figure 2A,B** show brain images of a female rat (98 g) at scan speeds of 4 s and 0.5 s, respectively. Sagittal sinus (SS) and transverse sinus (TS) are clearly visible in both the images. **Figure 2C,D** show photographs of the rat brain before and after removing the scalp over the brain area, respectively. PAT imaging was done non-invasively with intact skin and skull.

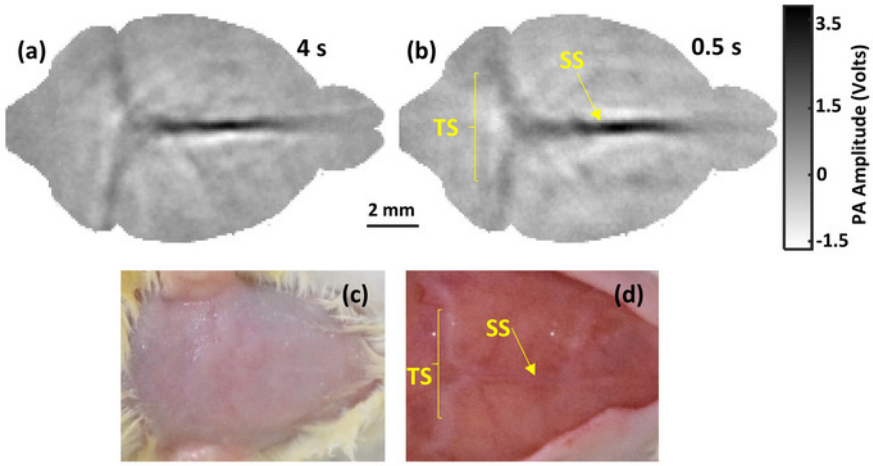

Figure 2: Non-invasive in vivo desktop PLD-PAT images. In vivo images of cortical vasculature at scan times of (**A**) 4 s and (**B**) 0.5 s. SS: sagittal sinus, TS: transverse sinus. (**C**) and (**D**) are photographs of the rat brain before and after removing the scalp, respectively. Please click here to view a larger version of this figure.

Before injecting ICG into the tail vein of the same rat, control data was acquired. After injecting ICG, PA data was acquired continuously for first 5 min with a 0.5 scan time. Then, PA data was acquired at ~2-3 min intervals with 0.5 s scan times each for the next 15-20 min. **Figure 3** shows the plot representing the increases in average PA signal in the sagittal sinus (SS) due to increases in optical absorption by ICG at 816 nm wavelengths, and subsequently, decreases over time.

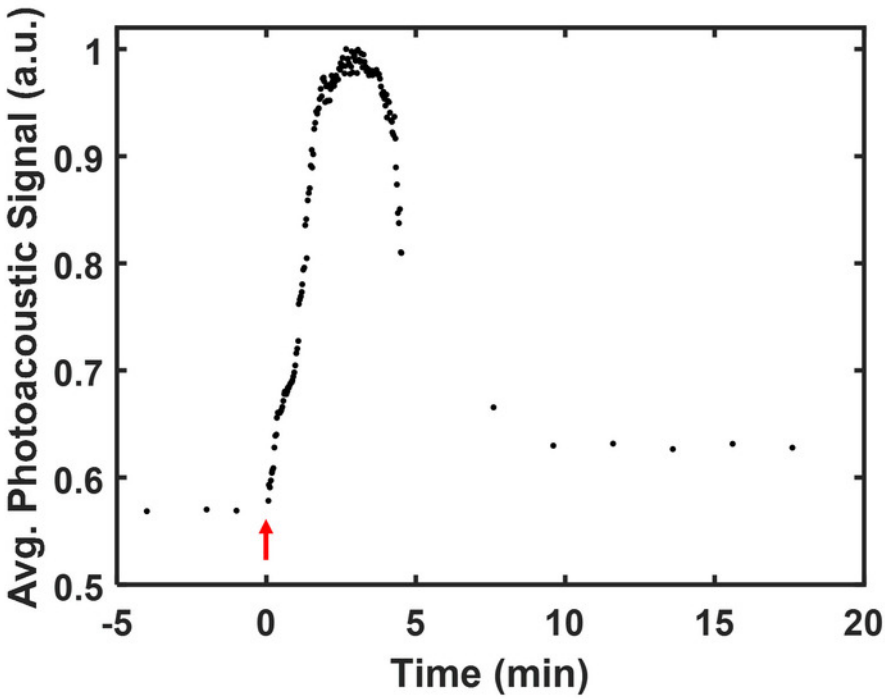

Figure 3: Pharmacokinetics of ICG. Pharmacokinetics of ICG showing the uptake and clearance process. The red arrow mark shows the time of injection of ICG into the tail vein. Please click here to view a larger version of this figure.

Discussion

This work presents a protocol to use a desktop PLD-PAT system for conducting experiments on small animals like rats for in vivo brain imaging and dynamic fast-uptake and clearance process of contrast agents like ICG. Bulky, expensive OPO-PAT systems take several minutes (2-5 min) to acquire a single cross-sectional in vivo image. A compact, low-cost, first generation portable PLD-PAT system provides single cross-sectional in vivo images in 5 s. In contrast, a high-speed, compact, low-cost desktop PLD-PAT system renders a high quality 2D cross-sectional in vivo image in just 0.5 s[26]. Here, the same desktop PLD-PAT system was demonstrated for fast in vivo dynamic brain imaging. Using this system, continuous monitoring of rapidly changing physiological phenomena is performed inside small animals for a fast rise and fall of PA signals due to ICG uptake and clearance processes. However, PLDs have a few limitations such as single wavelength generation, which forbids functional imaging. Additionally, multiple wavelength illumination is needed for acquiring the functional information. Also, imaging depth is limited due to a low per-pulse energy of PLD, which can be circumvented using exogenous photoacoustic contrast agents for enhancing the imaging depth.

While conducting the experiments using the desktop PLD-PAT system, certain precautions need to be taken: (a) due to the non-uniform beam profile of the PLD laser, an optical diffuser should be used at the laser output window, (b) it should be ensured that PLD laser beam is at the scanning center and that all SUTRs are facing towards the center of the PAT scanner, (c) care should be taken during anesthesia injection so that the surrounding organs like urinary bladder, kidneys, and intestines are not affected, (d) a proper amount of anesthesia mixture must be injected according to the weight of the animal, (e) during the procedure of trimming hair on the animal head, scratches on the scalp must be avoided, and (f) it must be ensured that the imaging plane of the rat brain is at the center of the acoustic reflector of the SUTRs. Troubleshooting may be needed if the image quality is low. Major applications of this system include high frame rate imaging (1 frame in 0.5 s), small animal brain tumor imaging, subcutaneous tumor imaging, and investigating biomaterials for potential PA contrast agents and therapeutic applications.

The maximum permissible exposure (MPE) safety limit for in vivo imaging is governed by the American National Standards Institute (ANSI) laser safety standards[29]. These safety limitations are dependent on laser pulse width, illumination area, exposure time, and illumination wavelength, as well as several other factors. Higher than a 700-1,050 nm wavelength range and maximum per pulse energy density on the skin surface should not exceed $20 \times 10^{2(\lambda-700)/1,000}$ mJ/cm^2, where λ (in nm) is the illumination wavelength. So, the MPE safety limit at a 816 nm wavelength of PLD laser used is ~34.12 mJ/cm^2. For continuous illumination of the laser over a period of t = 0.5 s, the MPE safety limit becomes $1.1 \times 10^{2(\lambda-700)/1000} \times t^{0.25}$ J/cm^2 (= 1.58 J/cm^2). The pulse repetition rate of the PLD was maintained at 2,000 Hz in all experiments. Over the course of a 0.5 s scan time, a total of 1,000 (0.5 x 2,000) pulses were delivered to the sample. This implies that per pulse, the MPE was 1.58 mJ/cm^2. The desktop PLD-PAT system delivers a per pulse energy of ~3.4 mJ. The laser energy density was maintained at ~0.17 mJ/cm^2 on the brain area as the laser beam expanded over a ~20 cm^2 area. This laser energy density was well below the ANSI safety limit over a period of 0.5 s. By reducing the pulse repetition rate, reducing the laser power, or expanding the laser beam, the ANSI laser safety limit for the desktop PLD-PAT system can be changed.

Disclosures

The authors have no relevant financial interests or potential conflicts of interest to disclose.

Acknowledgments

The research is supported by the Singapore Ministry of Health's National Medical Research Council (NMRC/OFIRG/0005/2016: M4062012). The authors would like to thank Mr. Chow Wai Hoong Bobby for the machine shop support.

References

1. Lin, L. *et al.* Single-breath-hold photoacoustic computed tomography of the breast. *Nature Communications.* **9** (1), 2352 (2018).
2. Upputuri, P. K., Pramanik, M. Fast photoacoustic imaging systems using pulsed laser diodes: a review. *Biomedical Engineering Letters.* **8** (2), 167-181 (2018).
3. Yao, J., Wang, L. V. Recent progress in photoacoustic molecular imaging. *Current Opinion in Chemical Biology.* **45,** 104-112 (2018).
4. Upputuri, P. K., Pramanik, M. Recent advances toward preclinical and clinical translation of photoacoustic tomography: a review. *Journal of Biomedical Optics.* **22** (4), 041006 (2017).
5. Yao, J., Wang, L. V. Photoacoustic microscopy. *Laser & Photonics Reviews.* **7** (5), 758-778 (2013).
6. Awasthi, N., Kalva, S. K., Pramanik, M., Yalavarthy, P. K. Image Guided Filtering for Improving Photoacoustic Tomographic Image Reconstruction. *Journal of Biomedical Optics.* **23** (9), 091413 (2018).
7. Kalva, S. K., Pramanik, M. Experimental validation of tangential resolution improvement in photoacoustic tomography using a modified delay-and-sum reconstruction algorithm. *Journal of Biomedical Optics.* **21** (8), 086011 (2016).
8. Pramanik, M. Improving tangential resolution with a modified delay-and-sum reconstruction algorithm in photoacoustic and thermoacoustic tomography. *The Journal of the Optical Society of America.* **31** (3), 621-627 (2014).
9. Xu, M., Wang, L. V. Universal back-projection algorithm for photoacoustic computed tomography. *Physical Review E.* **71** (1), 016706 (2005).
10. Wang, L. V., Hu, S. Photoacoustic Tomography: In Vivo Imaging from Organelles to Organs. *Science.* **335** (6075), 1458-1462 (2012).
11. Sivasubramanian, K., Periyasamy, V., Pramanik, M. Non-invasive sentinel lymph node mapping and needle guidance using clinical handheld photoacoustic imaging system in small animal. *Journal of Biophotonics.* **11** (1), e201700061 (2018).
12. Hu, S., Maslov, K., Wang, L. V. Second-generation optical-resolution photoacoustic microscopy with improved sensitivity and speed. *Optics Letters.* **36** (7), 1134-1136 (2011).
13. Stein, E. W., Maslov, K., Wang, L. V. Noninvasive, in vivo imaging of blood-oxygenation dynamics within the mouse brain using photoacoustic microscopy. *Journal of Biomedical Optics.* **14** (2), 020502 (2009).

14. Ku, G., Wang, X. D., Xie, X. Y., Stoica, G., Wang, L. V. Imaging of tumor angiogenesis in rat brains in vivo by photoacoustic tomography. *Applied Optics.* **44** (5), 770-775 (2005).
15. Ma, R., Taruttis, A., Ntziachristos, V., Razansky, D. Multispectral optoacoustic tomography (MSOT) scanner for whole-body small animal imaging. *Optics Express.* **17** (24), 21414-21426 (2009).
16. Zhou, Y. *et al.* A Phosphorus Phthalocyanine Formulation with Intense Absorbance at 1000 nm for Deep Optical Imaging. *Theranostics.* **6** (5), 688-697 (2016).
17. Li, L. *et al.* Single-impulse panoramic photoacoustic computed tomography of small-animal whole-body dynamics at high spatiotemporal resolution. *Nature Biomedical Engineering.* **1** (1), 0071 (2017).
18. Sivasubramanian, K., Pramanik, M. High frame rate photoacoustic imaging at 7000 frames per second using clinical ultrasound system. *Biomedical Optics Express.* **7** (2), 312-323 (2016).
19. Upputuri, P. K., Pramanik, M. Dynamic in vivo imaging of small animal brain using pulsed laser diode-based photoacoustic tomography system. *Journal of Biomedical Optics.* **22** (9), 090501 (2017).
20. Upputuri, P. K., Periyasamy, V., Kalva, S. K., Pramanik, M. A High-performance compact photoacoustic tomography system for in vivo small-animal brain imaging. *Journal of Visualized Experiments.* (124), e55811 (2017).
21. Upputuri, P. K., Pramanik, M. Pulsed laser diode based optoacoustic imaging of biological tissues. *Biomedical Physics & Engineering Express.* **1** (4), 045010-045017 (2015).
22. Arabul, M. U. *et al.* Toward the detection of intraplaque hemorrhage in carotid artery lesions using photoacoustic imaging. *Journal of Biomedical Optics.* **22** (4), 041010 (2016).
23. Daoudi, K. *et al.* Handheld probe integrating laser diode and ultrasound transducer array for ultrasound/photoacoustic dual modality imaging. *Optics Express.* **22** (21), 26365-26374 (2014).
24. Allen, J. S., Beard, P. Pulsed near-infrared laser diode excitation system for biomedical photoacoustic imaging. *Optics Letters.* **31** (23), 3462-3464 (2006).
25. Upputuri, P. K., Pramanik, M. Performance characterization of low-cost, high-speed, portable pulsed laser diode photoacoustic tomography (PLD-PAT) system. *Biomed Opt Express.* **6** (10), 4118-4129 (2015).
26. Kalva, S. K., Upputuri, P. K., Pramanik, M. High-speed, low-cost, pulsed-laser-diode-based second-generation desktop photoacoustic tomography system. *Optics Lett.* **44** (1), 81-84 (2019).
27. Kalva, S. K., Hui, Z. Z., Pramanik, M. Calibrating reconstruction radius in a multi single-element ultrasound-transducer-based photoacoustic computed tomography system. *J Opt Soc Am A.* **35** (5), 764-771 (2018).
28. Kalva, S. K., Pramanik, M. Use of acoustic reflector to make compact photoacoustic tomography system. *Journal of Biomedical Optics.* **22** (2), 026009 (2017).
29. American National Standard for Safe Use of Lasers. *ANSI Standard Z136.1-2007, NY.* (2007).

